

1
2
3
4
5
6
7
8
9
10
11
12
13
14
15
16
17
18
19
20
21
22
23

**The 23 June 2020, Mw 7.4 La Crucecita, Oaxaca, Mexico earthquake and tsunami: A
Rapid Response Field Survey during COVID-19 crisis**

María-Teresa Ramírez-Herrera^{*}, David Romero, Néstor Corona, Héctor Nava, Hamblet Torija,
Felipe Hernández M.

* Corresponding author full address: Laboratorio de Tsunamis y Paleosismología, Instituto de Geografía, Universidad Nacional Autónoma de México. Av. Universidad 3000, UNAM, Coyocán, Ciudad de México, C.P.04510, tramirez@igg.unam.mx.

Abstract

The 23 June 2020 La Crucecita earthquake occurred at 10:29 hr on the coast of Oaxaca in a Mw 7.4 megathrust event at 22.6 km depth, and triggered a tsunami recorded at Huatulco and Salina Cruz tide gauge stations and a DART off the coast of Mexico. Immediately after the earthquake, a rapid response effort was coordinated by members of the Tsunami and Paleoseismology Laboratory UNAM, despite the challenges by the COVID-19 pandemic crisis, a post-earthquake and post-tsunami field survey went ahead 2 days after the event. We describe here details of the rapid response survey focusing on evidence of vertical coseismic deformation, tsunami, geologic effects, and lessons from working in the field during the COVID-19 crisis. We surveyed 44 km along the coast of Oaxaca focusing on preselected sites. Because of COVID-19 pandemic, some local communities enforced rules of confinement. We solved most of the challenges faced during

24 this crisis by rapid networking with local organizations prior to surveying. We assessed
25 coseismic uplift by means of mortality caused by vertical displacement of intertidal organisms
26 and resurveying of bench marks, and measured tsunami runup using a laser ranger and GPS. Our
27 results show coastal uplift of 0.53 m near the epicenter, decreasing farther away from it, and up
28 to 0.8 m, the latest related to exposure of the coast. Our values of coastal uplift, ca. 0.53 m near
29 the epicenter, fit well with 0.55 m of uplift reported by tide gauge data at Huatulco. Coastal uplift
30 and low tide at the time of the event limited the tsunami inundation and runup on the Oaxaca
31 coast. Nevertheless, we found tsunami inundation evidence at four confined coastal sites
32 reaching a maximum runup of 1.5 m. The enclosed morphology of these sites determined higher
33 runup and tsunami inundation . Local coastal morphology effects are not detected in tsunami
34 models lacking detailed bathymetry and topography. This issue needs to be addressed during
35 tsunami hazard assessments.

36

37 1. Introduction

38

39 *23 June 2020 La Crucecita Earthquake and tsunami*

40

41 The 23 June 2020 La Crucecita earthquake occurred at 10:29 hr (local time), at 15.784° N and
42 96.120° W, and ruptured an estimated 30 km by 20 km (USGS) segment of the Mexican
43 subduction zone along the coast of Oaxaca in a Mw 7.4 megathrust event at 22.6 km deep (SSN,
44 2020), west of the intersection of the Tehuantepec ridge with the trench (Fig. 1). This earthquake
45 triggered a tsunami recorded at Huatulco and Salina Cruz tide gauges (SMN, 2020), and a DART
46 off the coast of Mexico (PTWC, 2020). A tsunami alert by the Pacific Tsunami Warning Center

47 (PTWC) was issued at 10:39 hrs. The earthquake left at least 10 people dead on the Oaxaca
48 highlands and no tsunami damage was reported. Immediately after the earthquake, a rapid
49 response effort was coordinated by members of the Tsunami and Paleoseismology Laboratory,
50 Instituto de Geografía, UNAM and despite the challenges by the COVID-19 pandemic crisis, a
51 post-earthquake and post-tsunami field survey went ahead 2 days after the event. We describe
52 here details of the rapid response survey, challenges faced during a COVID-19 crisis, and results
53 on measurements of coseismic deformation, tsunami runup observations, and other geologic
54 effects generated by the earthquake.
55

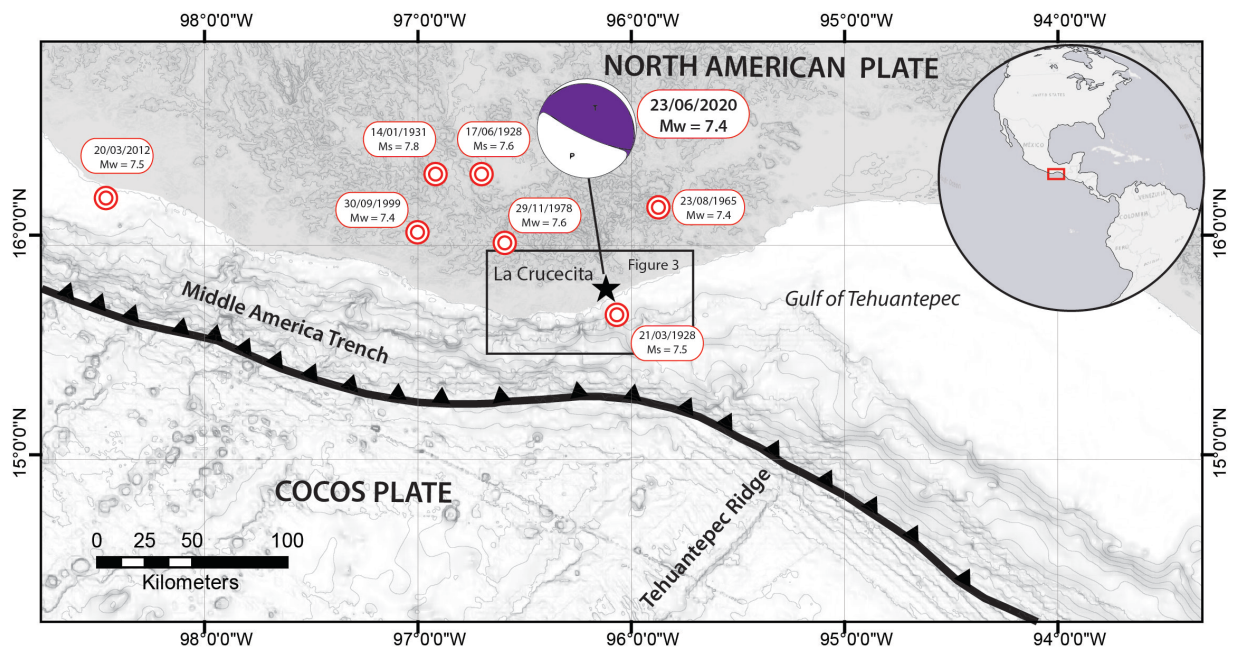


Figure 1. Tectonic and earthquake setting. Red bullseye – Mw > 7 earthquakes in the Oaxaca region (SSM, 2020b); star – 23 June 2020 epicenter (SSM, 2020a); Moment tensor of the 23 June 2020 earthquake (USGS (2020)).

56
57 Figure 1. Tectonic and earthquake setting. Red bullseye – Mw > 7 earthquakes in the Oaxaca
58 region (SSM, 2020b); star – 23 June 2020 epicenter (SSM, 2020a); Moment tensor of the 23
59 June 2020 earthquake (USGS (2020)).

60

61

62 *Tectonic and earthquake setting*

63

64 The 23 June 2020 La Crucecita earthquake nucleated at the Cocos-North America plate
65 boundary (Fig. 1) with a M_w 7.4 (SSN, 2020a). Convergence rates in this sector of the Mexican
66 subduction zone are near 70 mm/yr (DeMets et al, 2010). The megathrust event (strike= 266.8 ,
67 dip= 17.2, slip= 60.5) reached a maximum slip of 3.2 m slip (SSN, 2020a), although the USGS
68 reported 7.5 m maximum slip (USGS, 2020). The Servicio Mareográfico Nacional (SMN, 2020)
69 reported a +0.55 m land-level change recorded at the HUAT tide gauge. More than 7,000
70 aftershocks were recorded by July 14, 2020, the largest of which had a M_w 5.5 and occurred at
71 21:33 hr on 23 June 2020. Large earthquakes, $M_w > 7$, are common in this region and several
72 have been recorded during the last and this centuries (Kostoglodov and Ponce, 1994; Ramírez-
73 Herrera et al., 1999; SSN, 2020b). Earthquakes of this magnitude have rupture areas of about 70
74 x 35 km (length x width) according to the USGS (2020), and earthquakes such as the M_w 6.4,
75 the Puerto Angel earthquake of 1998 produced coastal uplift (Ramírez-Herrera and Zamorano,
76 2002).

77

78 *Tsunami*

79

80 The instrumental record indicates that the 1978 M_w 7.7 (Sanchez and Farreras, 1993) and the
81 2012 M_w 7.5 produced tsunamis (Ramírez- Herrera, personal comm.) (Fig. 1). However,
82 historical events registered in archives indicate that great earthquakes and tsunamis have

83 occurred in historical time and geological evidence of the 1787 and probable predecessor in 1537
84 have flooded the southwest coast of Mexico (Ramírez-Herrera et al., 2020). However, because of
85 the short instrumental record, tsunami hazard has been minimized and incorrectly evaluated on
86 the Pacific coast of México.

87

88 *Coastal land level changes and mortality of intertidal organisms*

89

90 Sudden coastal uplift has been documented using mortality of intertidal organisms and upper
91 subtidal algae to estimate coseismic land-level changes particularly in subduction zones (e.g.
92 Plafker, 1964; Johansen, 1971; Bodin And Klinger, 1986 ; Plafker and Ward, 1992; Pelletier et
93 al, 2000; Ortlieb et al., 1996; Ramírez-Herrera and Zamorano, 2002; Lagabrielle et al., 2003;
94 Farias et al., 2010; Melnick et al., 2012). Vertical zonation of intertidal species depends on
95 factors associated with the tidal cycle (Lunning, 1990; Ortlieb et al. 1996).

96

97 Sudden uplift by earthquakes produces mortality among intertidal organisms, normally life
98 dependent on the time they are exposed during low tides. Intertidal organisms mortality is
99 commonly accompanied by whitening (bleaching) of the dead organism generating a white belt
100 that differentiates clearly from the pinkish color of living organisms right below (Johansen,
101 1971; Ortlieb et al., 1996).

102

103 We used intertidal organisms to evaluate coseismic coastal uplift associated with the 23 June
104 2020 Oaxaca earthquake using coralline algae and invertebrate species living at intertidal and
105 upper subtidal, and in few cases the supralitoral, marine habitats (Ramírez-Herrera & Zamorano

106 2002, Castilla et al. 2010). The intertidal habitat is between the highest and the lowest levels of
107 the tidal range. The biological communities in this habitat may be adapted to be submerged and
108 emerged periodically due the influence of the daily tides. The upper subtidal habitat begins
109 below the lowest level of the intertidal range, and the species inhabiting there are permanently
110 submerged. Supralittoral habitat is submerged only occasionally during the highest spring tides
111 and mainly is influenced by the sea waves and the marine breezes (Tait & Diper 1998).

112

113 *Rapid response*

114

115 The 23 June 2020 earthquake and tsunami occurred during the COVID-19 pandemic crisis,
116 despite this we coordinated a rapid response effort and a post-earthquake and post-tsunami field
117 survey went ahead 2 days after the event. We contacted a local network of people in positions
118 that allowed us rapid access to surveyed sites before the evidence was obliterated by rain and/or
119 human activity.

120

121 2. Field Survey

122

123 Two days after the 2020 Oaxaca earthquake, we started a five-day survey, despite challenges and
124 restrictions imposed by the COVID-19 pandemic, which were related to safe flight travel,
125 confinement, closed hotels and restaurants, to rapidly measure tsunami runup and coastal
126 coseismic deformation, marked by the elevation of bleached intertidal organism belts, and
127 surveying of benchmarks by SMN. We focused at the Huatulco bays region on 15 locations
128 along 44 km of the coast (Fig. 1). The width of bleached intertidal organisms and upper subtidal

129 algae belt, marked by the top and base of the belt, was measured directly on the bleached belt
130 using a metric tape on exposed to waves rocky outcrops and on exposed coral reefs, and only few
131 measurements were made with laser rangefinder when sites were not reachable. We measured
132 tsunami runup by means of marks above the high tide level using a laser rangefinder. Laser
133 rangefinder precision on short distances, < 100 m, is < 5 cm, and measures directly on the
134 exposed rock with tape had less than 0.5 cm error. We photographed all measured sites and
135 located them with a GPS recording time to assess tide levels at the time of measurement. We
136 also surveyed coral reefs using a drone TBS Discovery to map the bleached coral reef areas.

137

138 Tide gauge data from Servicio Mareográfico Nacional (SMN) at Huatulco station (see Table S1
139 of Supplemental material) were used to assess the living position and mortality of intertidal
140 organisms used in this study to estimate coastal uplift.

141

142 3. Observations and results

143

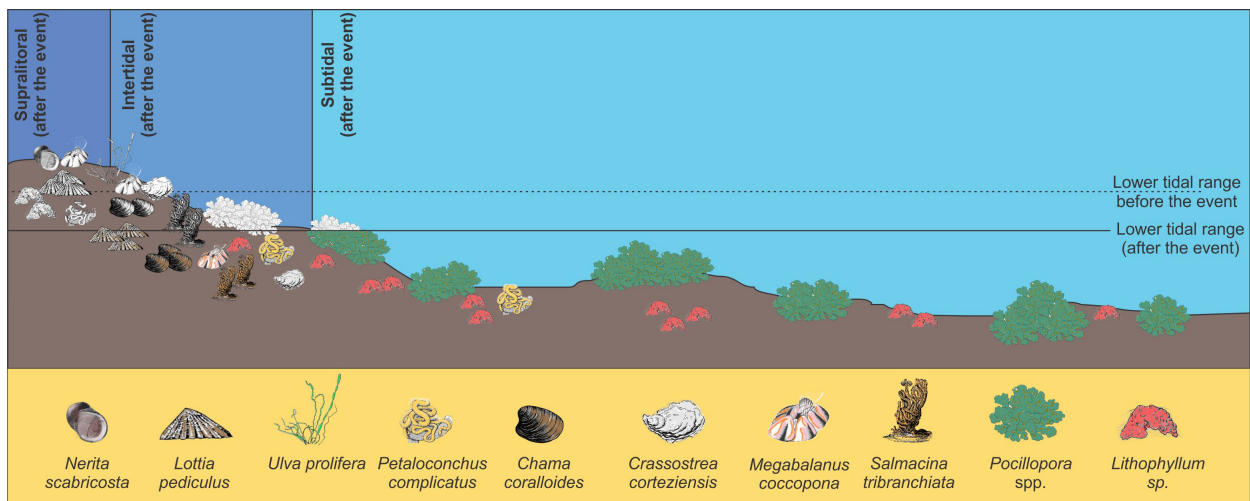
144 *Bleaching or mortality of intertidal organisms*

145

146 We identified several species of bleaching organisms and their taxonomy as well as their habitat
147 summarized in Table S2 of the Supplemental material. We also use corals from coral reefs that
148 showed signs of bleaching and emergence. Based on collected samples of organisms and
149 photographs taken in the field, the taxonomic identity of all species were verified with literature
150 available for the area and the World Register of Marine Species (WORMS). Their taxonomy is
151 also summarized in Table S2 and Figure S1 of Supplemental material. In summary, the

152 organism identified and used in this study are: a) green algae *Ulva prolifera*, b) gastropod *Nerita*
153 *scabricosta*, c) gastropod *Lottia pediculus*, d) bivalve *Crassostrea corteziensis*, e) vermetid
154 *Petalococonchus complicatus*, f) polychaete *Salmacina tribranchiata*, g) crustacean *Amphibalanus*
155 *eburneus*, h) bivalve *Chama coralloides*, i) crustacean *Megabalanus coccopoma*, j) coralline
156 algae *Lithophyllum* sp., k) stony coral *Pocillopora verrucosa* and l) stony coral *Pocillopora*
157 *damicornis*. Vertical zonation of the organisms used in this study is shown in Figure 2 on and
158 Table S2 of Supplemental material. Mean tidal range is 0.89 m, extreme tidal range is 1.02 m,
159 and maximum extreme tidal range is 1.02 m at this stretch of the Oaxaca coast (Grivel & Grivel,
160 1993).

161



162 Figure 2. Vertical zonation of the organisms used in this study.

163 Figure 2. Vertical zonation of the organisms used in this study

164

165 *Coastal Uplift*

166

167 We measured the bleaching belt of organisms indicative of mortality at 15 locations along the

168 Oaxaca coast (Fig. 3). We collected several measurements at different sites, where possible

169 more than one measurement was registered at each location to have a statistically representative
170 value. Only four sites showed values that did not satisfy the quality criteria (Ortlieb et al., 1996).
171 These values were measured on sites on enclosed tide pools; two high values were measured in
172 an estuary, and one site showed exposed corals difficult to measure from a far distance.

173

174 Our results on measuring the bleaching belt of intertidal organisms indicates that coastal uplift
175 produced by the Mw 7.5 Huatulco earthquake extended along 44 km between San Isidro west of
176 the epicenter, and Barra de la Cruz east of the epicenter (Fig. 3). The further west and east of the
177 epicenter showed low to none evidence of intertidal organisms mortality. The coastal stretch at
178 Playa El Violin, Playa La Yerbabuena, Playa Pescadores-Quinta Real, Fonatur dock, and Playa
179 Pescadores- Santa Cruz showed clear evidence of widespread intertidal organism bleaching belt
180 (OBB). The width of OBB ranged from 0.1 up to 0.8 m along the surveyed area. However, the
181 largest values do not fit the criteria for assessing coastal uplift and are reflecting amplification of
182 the OBB by local features such as coastal morphology (intertidal pools, estuaries, wave splash
183 and far distance features). Those values are excluded from the final estimate of coastal uplift.

184

185 The OBB width at FONATUR dock ranged from 0.4 to 0.54 m, and a mean of 0.47 m (Fig. 3
186 and Fig. 4). At Playa Pescadores-Santa Cruz the OBB width values ranged from 0.5 to 0.56 m
187 with a mean of 0.535 m. We consider these values to be representative of the uplift in this area.
188 At Marina Chahue values range from 0.2 to 0.4, mean value is 0.28 m. We excluded the largest
189 value of 0.8 m because it reflected the amplification of the local intertidal pool. At Playa
190 Pescadores-Quinta Real we measured a relatively high value of 0.6 m. This is caused by the
191 effect of a narrow channel fenced by two breakwater structures on both sides. Further to the NE,

192 at la Bocana, the mean value of OBB width was 0.37 m. At Zimatan-Laguna Las Garzas beach,
193 values range from 0.2 to 0.3 m., which reflects the decrease in uplift away from the area of the
194 epicenter. At Zimatan-Laguna Las Garzas river mouth, values were high, mean value 0.77 m.
195 This site does not reflect the real deformation because the vertical distribution of intertidal
196 organisms here is influenced by specific characteristics of the location (Ortlieb et al, 1996). At
197 Barra de La Cruz, we were not granted access to the beach due to COVID-19 lockdown
198 measures taken by the locals. To the west of the epicenter, at Playa Yerbabuena (SEMAR)
199 values ranged from 0.2 to 0.53 m, with a mean value of 0.32 m. Playa Violin showed OBB
200 width ranged from 0.29 to 0.57 m, mean value is 0.42 m (Fig. 3 and Fig. 4). At Bahía El Órgano,
201 representative values ranged from 0.2 to 0.4 m. We did not include an extremely high value of
202 0.8 m produced by the local site effect (an enclosed tidal pool). Playa Riscalillo showed coral
203 reef bleached width ranging between 0.10 to 0.20 m. San Agustin bay also showed coral reef
204 exposed above mean sea level, however the distance to the reef precluded us from taking a
205 precise measure, thus we excluded the 0.70 m value that is not representative. At Playa del Amor
206 values ranged from 0.10 to 0.20 m which are consistent with an expected decrease of OBB width
207 away from the epicenter. The furthest west location, at San Isidro evidence was scarce and the
208 belt measured at the mouth of an estuary showed values in between 0.15 and 0.20 m, reflecting
209 site increment effects. The latest suggests that uplift here was minimal, perhaps less than a few
210 centimeters. We did not expect to find evidence further to the west since last site only showed
211 patchy evidence of OBB.

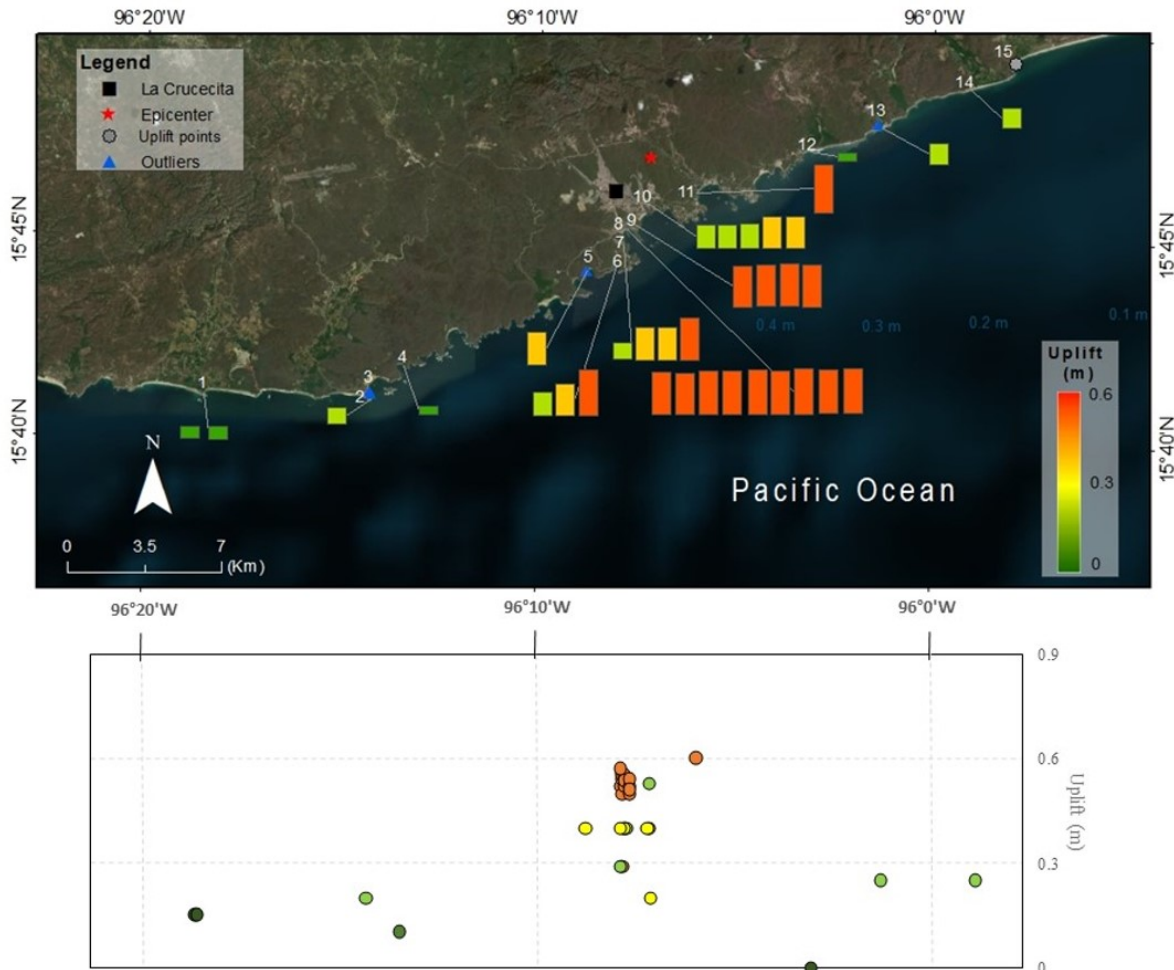


Figure 3. Coseismic uplift generated by the La Crucecita Mw 7.4, 23 June 2020, earthquake. Bars indicate the width (m) of the organisms bleached belt (OBB) at 15 locations along 44 km of coastal stretch: 1. San Isidro, 2. Playa del Amor, 3. San Agustín, 4. Bahía Riscalillo, 5. Playa el Órgano, 6. Playa el Violín, 7. Playa Yerbabuena – SEMAR, 8. Playa Pescadores, 9. Fonatur dock, 10. Marina Chahué, 11. Playa Pescadores – Quinta Real, 12. La Bocana Río Copalita, 13. Río Zimatán, 14. Zimatán – Laguna las Garzas, 15. Barra de la Cruz. Blue triangles – sites with values > 0.5 m. Please see the text for explanation.

212

213 Figure 3. Coseismic uplift generated by the La Crucecita Mw 7.4, 23 June 2020, earthquake.

214 Bars indicate the width (m) of the organisms bleached belt (OBB) at 15 locations along 44 km of

215 coastal stretch: 1. San Isidro, 2. Playa del Amor, 3. San Agustín, 4. Bahía Riscalillo, 5. Playa el

216 Órgano, 6. Playa el Violín, 7. Playa Yerbabuena – SEMAR, 8. Playa Pescadores, 9. Fonatur

217 dock, 10. Marina Chahué, 11. Playa Pescadores – Quinta Real, 12. La Bocana Río Copalita, 13.

218 Río Zimatán, 14. Zimatán – Laguna las Garzas, 15. Barra de la Cruz. Blue triangles – sites with
219 values > 0.5 m. Please see the text for explanation.

220

221 Figure 3 summarizes the distribution and amount of coseismic uplift estimated from OBB. We
222 have used all values and mean values to graphically represent the width of the OBB. These
223 values are estimates of the land level change, i.e. coseismic uplift by the 23 June 2020
224 earthquake. We use only values that best represent the uplift and excluded values from locations
225 that were influenced by site effects. The maximum estimated uplift was identified at Playa
226 Pescadores- Santa Cruz, FONATUR duck, Playa Pescadores-Quinta Real, and Playa El Violin.
227 From this area on, to the west and northeast farther away from the earthquake epicenter, values
228 of uplift tend to decrease. Uplift represented by mortality of intertidal organisms extended about
229 40 km along the coast. We are not sure about the extent of uplift further NE since we were
230 prevented access to locations from Barra de La Cruz on, however we already observed a
231 decrease in uplift at the nearest location. The general pattern of coseismic uplift indicated by the
232 OBB width suggests greater land vertical motion closer to the epicenter.

233



Figure 4. Mortality of intertidal organisms caused by sudden land uplift shown by a bleaching belt of intertidal organisms. UL = Upper limit and LL Lower limit of organism bleached belt. a) La Bocana Río Copalita , b) San Isidro, c) Bahía Riscalillo – aerial view of patches of bleached coral reef, d) Marina Chahué, e) Playa el Violín, f) Bleached coral reef at Bahía Riscalillo g) Playa Yerbabuena – SEMAR – bleached coral, h) Playa Pescadores, i). Detail of bleached belt at Playa Pescadores.

235 Figure 4. Mortality of intertidal organisms caused by sudden land uplift shown by a bleaching
236 belt of intertidal organisms. UL = Upper limit and LL Lower limit of organism bleached belt.
237 a) La Bocana Río Copalita , b) San Isidro, c) Bahía Riscalillo – aerial view of patches of
238 bleached coral reef, d) Marina Chahué, e) Playa el Violín, f) Bleached coral reef at Bahía
239 Riscalillo g) Playa Yerbabuena – SEMAR – bleached coral, h) Playa Pescadores, i). Detail of
240 bleached belt at Playa Pescadores.

241
242 We measured the elevation of two benchmarks set by the SMN to have a different data parameter
243 and being able to compare and determine with more parameters land-level changes. The first
244 bench mark (BN20HUA01) is located at the Fonatur dock next to the tide gauge and the second
245 bench at the park kiosk (BN20HUA02). Bench mark BN20HUA01 showed 0.528 m uplift and
246 BN20HUA02 experienced 0.491 m uplift after the 23 June 2020 earthquake.

247
248 *Tsunami*

249
250 A tsunami was generated by the Mw 7.4 La Crucecita earthquake. The earthquake occurred at
251 10:29 hr local time. The SMN Huatulco tide gauge registered a maximum tsunami amplitude of
252 0.61 m at 13:12 hr local time, and at Salina Cruz tide gauge station with a maximum amplitude
253 of 1.394 m at 12:34 hr local time (Fig. S2 Supplemental material). According to the registered
254 tide gauge data, the sea started retreating at 10:30 hr reaching a maximum retreat of -1.273 m at
255 10:36 hr. The SMN Huatulco interpretation suggests that the tsunami initiated at 11:12 hr
256 reaching a maximum amplitude of 0.61 m at 13:12 hr, and ending at 18:06 hr (Fig. S2
257 Supplemental material)

258
259
260
261
262
263
264
265
266
267
268
269
270
271
272
273
274
275
276
277
278
279
280

However, we observed several videos recorded by static camera devices at the FONATUR dock and estimated that the sea started to retreat approximately 5 to 7 minutes after the earthquake (the retreat could have started earlier since power went off and 5 minutes of record were lost), with turbulence and sediment in suspension, and reached the lowest level 11 minutes after the earthquake. The sea apparently made a return, with relative strong energy and speed, 13 minutes after the earthquake, i.e. at approximately between 10:43 or 10:45 hr local time. At 10:47 again the sea retreated and reached a maximum height by 10:48 hr to again reach an apparent lower level than the one the sea showed before the earthquake.

According to social media and witnesses reports, the sea retreated almost immediately after the earthquake but did not cause extensive inundation nor damage was reported in coastal cities. Witnesses reported sea return but emphasized it never reached the sea level previous to the earthquake. After the earthquake some coastal residents started a timely evacuation to higher ground after seeing the sea retreat, however not all coastal residents evacuated. No damage nor deaths were reported due to the tsunami. The Mexican Tsunami Warning Center (CAT – Centro de Alertas de Tsunami) issued a tsunami alert, however none of the coastal residents we interviewed were aware of the tsunami warning other than the earthquake itself.

Tsunami marks left on the shore were scarce on the surveyed sites. We expected to find only a few marks after looking at tide gauge data reports of the 23 June 2020 tsunami on Huatulco and Salina Cruz stations, also because at the time of earthquake and tsunami the tide level was low (-0.582 m), and as explained above we observed a bleaching belt of intertidal organisms

281 indicative of coastal uplift. However, we located sand and cobbles beyond high tide mark on
282 boat ramps, organic debris (broken coral) higher than the highest tide mark on a beach, and other
283 organic debris, at four sites along 44 km of the surveyed coast. At Playa El Violin we found a
284 line of broken corals from a local coral reef located higher than the highest tide mark, indicative
285 of tsunami runup ~ 0.9 m. This narrow and confined bay faces to the SW (Fig. 5). The second
286 site at Marina Chahue, with a very narrow entrance to the Marina (Fig. 5), showed a tsunami
287 mark made of sand and cobbles on a concrete ramp next to fuel pumps, and the measured runup
288 was ~ 1.07 to 1.37 m. Playa Pescadores (Quinta Real) is an extremely narrow channel facing SE,
289 confined by groins that might have increased the tsunami runup up to ~ 1.57 m. La Yerbabuena
290 beach at the boat ramp, confined by a dock and a cliff, also showed a tsunami mark made of
291 sand and cobbles with a runup of 0.99 m (Fig. 5). All these sites have in common being narrow
292 and confined. We explained the absence of tsunami marks by: 1) low tide at the time of tsunami
293 and 2) land uplift of this portion of the coast caused by the earthquake, that decreased the size of
294 the tsunami. The few tsunami marks left on the shore can be explained by the local morphology
295 of these sites: very narrow confined channels and likely the bathymetry of a narrow entrance bay.
296 These local effects cannot be envisaged in tsunami models due to the gross topography
297 bathymetry used in modeling, and this is an issue that requires to be addressed when using
298 modeling in tsunami hazard assessment.

299

300



Figure 5. Tsunami runup marked by debris at four locations along the study area. a) El Violín Beach, b) Marina Chahué, c) Playa Yerbabuena – SEMAR.

301

302 Figure 5. Tsunami runup marked by debris at four locations along the study area. a) El Violín

303 Beach, b) Marina Chahué, c) Playa Yerbabuena – SEMAR.

304

305

306

307 *Other Geologic effects (liquefaction, fissures, landslides)*

308

309 We observed near the coast several geologic effects associated with the Mw 7.4 earthquake's
310 ground shaking, with PGA 20% g and PGV 41.4 cm/s, intensity VIII near the epicenter (USGS,
311 2020) (Fig. 1). Rockfalls and landslides were common along coastal highways and on some
312 slopes, however their size was relatively small. Lateral spreading, fissures on the ground and
313 beaches were common. Liquefaction (sand boils) was focused near estuaries, river mouths, and
314 lagoons (Fig. 6). Most of the landslides were reported on the Oaxaca highlands and these were
315 not included in the scope of this survey. It is worth mentioning that the current rainy season at
316 the time of the earthquake in Oaxaca, Mexico, most probably increased slope failures.

317

Fissures



Soil liquefaction



Landslides



Figure 6. Other Geologic effects: liquefaction, fissures, landslides caused by La crucecita earthquake of 23 June 2020. a) Playa Pescadores – Quinta Real, b), c) and g) Zimatán-Laguna las Garzas, d) La Bocana Río Copalita, e), f) Boulevard Chahué.

318

319

320 Figure 6. Other Geologic effects: liquefaction, fissures, landslides caused by La crucecita
321 earthquake of 23 June 2020. a) Playa Pescadores – Quinta Real, b), c) y g) Zimatán-Laguna las
322 Garzas, d) La Bocana Río Copalita, e), f) Boulevard Chahué.

323

324 Buildings along the coast apparently had very few damage. Although beyond the scope of this
325 survey, we noticed mainly a few 3 to 4-store buildings that showed structural damage. Most of
326 the hotels and houses close to the beach responded well with minor damage (broken roof tiles).

327

328 *Surveying during COVID-19 crisis*

329

330 Field survey was carried out in the state of Oaxaca during the COVID-19 pandemic crisis. Santa
331 María Huatulco was selected as the operation center, since this was the area of the La Crucecita
332 earthquake epicenter. On the arrival day, the epidemiological panorama of the coastal region
333 showed 170 COVID-19 active cases, and at Santa María Huatulco only 7 COVID-19 cases. We
334 followed all recommendations regarding prevention during the course of the post-earthquake and
335 tsunami survey: all the participants involved wore masks, the use of alcohol gel, frequent hand
336 washing and keeping a 1.5 m distance. Only one vehicle was used during the survey, which was
337 washed and disinfected every day, the interaction with people during field work was always
338 respecting a safe distance and the use of masks, in addition to the permanent vigilance for the
339 appearance of any symptoms by the team members (Fig. 7).

340

341

342



Figure 7. Surveying during COVID-19 crisis. a) Arrival at Huatulco airport and reception by the Bomberos de Oaxaca (Oaxaca Firemen). b) SEMAR (Mexican Navy) vessel used to reach inaccessible by land coastal locations. c) Instructions and discussion with SEMAR members keeping a safe distance and wearing masks. d) Sign at Barra de La Cruz indicating restricted access to the town due to COVID-19 confinement.

343

344 Figure 7. Surveying during COVID-19 crisis. A) Arrival at Huatulco airport and reception by the

345 Bomberos de Oaxaca (Oaxaca Firemen). b) SEMAR (Mexican Navy) vessel used to reach

346 inaccessible by land coastal locations. c) Instructions and discussion with SEMAR members

347 keeping a safe distance and wearing masks. d) Sign at Barra de La Cruz indicating restricted

348 access to the town due to COVID-19 confinement.

349

350 We faced a few challenges and restrictions imposed by the COVID-19 pandemic. Prior to

351 traveling we contacted our local network in Huatulco, Oaxaca, to rapidly get access to sites along

352 the coast. Traveling to the coast in a rapid way required flying in a packed airplane with no

353 empty seats in between passengers. Due to the confinement in some towns most hotels and

354 restaurants were closed, however we had the support of the La Crucecita, Huatulco, Firemen

355 (Bomberos de Oaxaca), and FONATUR (the Federal office for tourist affairs) who kindly
356 arranged for us to use a truck and hotel reservations during the survey. To get rapid access to less
357 accessible sites, the Navy local office aided in using a Navy boat (Fig. 7). All of this was
358 arranged previous to arrival by our local contact with Oaxaca Firemen. It is therefore very
359 important to have a good network and work with locals in times of crisis for a rapid evaluation of
360 earthquake and tsunami effects.

361

362 During the survey, we always respected the local practices and actions of containment because of
363 the pandemic. We first talked with the local authorities at checkpoints to ask for access, as it was
364 the case in the community of La Bocana and Copalita. However, we could not have access to
365 some places, such as the community of Barra de La Cruz where access to anyone outside the
366 community was prohibited (Figure 7). We solved this situation by visiting the nearest possible
367 site to make observations.

368

369 Summary and Discussion

370

371 The 23 June 2020 La Crucecita earthquake produced coastal uplift recorded by the extent of
372 mortality of intertidal organisms caused by sudden vertical motions. A white belt of dead
373 organisms appeared at several sites along the coast and was already visible by the second day
374 after the earthquake. The width of this belt varied along the coast, generally showing higher
375 values near the epicenter and decreasing further away. Evidence of coastal deformation was
376 observed between San Isidro and Zimatan (Fig. 3), that we considered the along-strike extent of
377 the 23 June 2020 La Crucecita earthquake rupture of ca. 40 km. Our results based on the

378 interpretation of most representative values that fulfilled the criteria explained above, show
379 coastal coseismic uplift of 0.53 m near the epicenter and farther away decreasing to 0.10 m. The
380 bleached belt of intertidal organisms is a reliable estimate of the uplift produced by the 23 June
381 2020 La Crucecita earthquake. Other phenomena such as extremely low tide and El Niño events
382 cannot explain the mortality of intertidal organisms since, firstly we surveyed sites that had
383 experienced low tide sequences and 2020 had no El Niño event on the coast of México.
384 Furthermore, fishermen and locals pointed to the “no return of the sea to its normal level after the
385 earthquake”, i.e. coastal land level change, and to the mortality of coral reefs and other intertidal
386 organisms. Furthermore, we corroborated our results with measurements of two geodetic SMN
387 benchmarks at Santa Maria Huatulco near la Crucecita. Our results using benchmarks height
388 measurements confirm coastal uplift of 0.528 m on the coast and 0.491 m slightly inland (Fig. 3).
389 Also, we used the SNM tide gauge data (Fig. S1 of Supplemental material) and SNM report that
390 indicates coastal uplift of 0.55 m. Therefore the observed bleached belt reliably represents
391 coseismic uplift produced by the 23 June 2020 La Crucecita earthquake. We suggest that the use
392 of organisms sudden mortality aids in a rapid survey of earthquake deformation along the coast.
393
394 Tsunami evidence was scarce and our measurements of tsunami runoff on the surveyed coastal
395 stretch showed 0.9 m and a maximum runoff of 1.5 m at four confined coastal sites. The scarcity
396 of tsunami evidence can be explained by several factors. Firstly, it was raining during and the
397 night after the event, thus evidence such as debris are not perennial and could be easily washed
398 away by rain. Secondly, the tide level at the tsunami arrival was low (-0.58 m), which also
399 contributed limited tsunami inundation and runoff at the coast. Finally, coastal uplift of ca. 0.53
400 to 0.10 m, also limited tsunami inundation and runoff. Despite all of the explained above, we

401 observed evidence at four coastal sites with confined coastal morphology. Tide gauge records,
402 testimonies by locals, and video recordings also support evidence of the sea retreat and energetic
403 sea return, even if with relatively low tsunami heights, a few minutes (~5 to 7 minutes) after the
404 earthquake.

405

406 Thus, it is important to remember and emphasize that historical and prehistorical earthquakes
407 produced great tsunamis on the Mexican Pacific coast, such as the 1787 event and the possible
408 predecessor of 1537 (Ramírez-Herrera et al., 2020). Instrumental data unfortunately do not
409 capture in their short record (ca. 100 years) in Mexico all tsunamigenic events, nor all
410 earthquakes produced coastal uplift on the Pacific coast of Mexico. For instance, the 1995 Mw
411 8.0 Colima-Jalisco earthquake produced coastal subsidence and a significant tsunami with run-up
412 height of 5.1 m (e.g. Pacheco et al., 1997; Borrero et al., 1997; Trejo-Gómez et al., 2015). Even
413 when earthquakes produced coastal uplift, as it happened during the 19 September 1985 Mw 8.1
414 (Bodin and Klinger, 1986) and 20 September 1985 Mw7.5 earthquakes, two tsunamis flooded
415 the coast of Michoacan and Guerrero, Mexico (Sanchez and Farreras, 1993) leaving geologic
416 evidence (Ramírez-Herrera et al., 2012). It is also possible that shallow events near the trench
417 might cause coastal subsidence and large tsunamis such as the 1787 event (Ramírez-Herrera et
418 al., 2020) and the more recent 1995 Mw 8.0 Colima-Jalisco earthquake (Pacheco et al., 1997;
419 Hjörleifsdóttir et al., 2018). Tsunami modeling exercises may aid in estimating tsunami
420 amplitudes, however due to the lack of detailed bathymetry and topography, local coastal
421 morphology effects are missed in models. Thus an effort should be made to produce bathymetric
422 data near the coast to have reliable tsunami models. This and tsunami education programs are of
423 most importance in tsunami hazard prevention to create tsunami resilient coastal communities.

424

425 Finally, our lesson from working during the Covid-19 pandemic crisis is that it is crucial to have
426 a local network of collaborators who facilitate a rapid response during post-earthquake and
427 tsunami surveys by aiding in getting access to localities and sites affected by this phenomena,
428 assists in logistics, help in understanding and respecting local practices by communities that in
429 turn cooperate in describing these phenomena.

430

431 Data and Resources

432 Supplemental material includes Table S1 presenting tide gauge data from Servicio Mareográfico
433 Nacional (SMN) at Huatulco station. Data were used to assess living position and mortality of
434 intertidal organisms.

435

436 Table S2 provides data on the taxonomic identity and vertical zonation of organisms used in this
437 study.

438

439 Figure S1 includes details, taxonomy, and photographs of the organisms used in this study.

440 Figure S2 shows the Huatulco tide gauge data interpretation of land-level vertical displacement
441 and tsunami amplitude after the 23 June 2020 earthquake.

442

443 *Acknowledgments*

444

445 This work was supported by Instituto de Geografía, Universidad Nacional Autónoma de México
446 and CONACYT-SEP 284365 granted to Ramírez-Herrera. We thank the following people and

447 Institutions for logistic help during the survey: Bomberos Oaxaca - Lic. Manuel A. Maza
448 Sánchez; Secretaria de Marina - Sector Naval Huatulco- Contralmirante CGDEM Procoro Juan
449 Trinidad García and Capitán Juan Solís Guillén, Secretaría de Seguridad Pública- Lic. Raul
450 Ernesto Salcedo Rosales; Secretaria de Turismo - Delegación Regional Huatulco - Lic. Raúl
451 Sinobas Solís, Fonatur - Delegación regional CIP Huatulco - Ing. Ramón Sinobas Solís,
452 Capitanía del Muelle de Cruceros – Cap. Ángulo, FONATUR – Mario Harrigan. Víctor Vargas
453 helped with figure drafting. Diego Melgar shared preliminary slip, vertical deformation, and
454 tsunami amplitude models. We thank the coastal communities of Oaxaca visited during this post-
455 earthquake and post-tsunami field survey for kindly giving access, sharing their memories and
456 videos of the events.

457

458 **References**

459

460 Bodin, P., & Klinger, T. (1986). *Coastal uplift and mortality of intertidal organisms caused by*
461 *the September 1985 Mexico earthquakes*. *Science*, 233, 1071–1073.

462 Borrero, J., Titov V., Ortiz M., , Synolakis C. (1997). Mexican Earthquake Generates Tsunami,
463 New Data, and Unusual Photos. *Earth in Space*, vol. 9, no. 7, p. 5-8, 1997 American
464 Geophysical Union. Retrieved July 21, 2020
465 from http://www.agu.org/sci_soc/eisborerro.html

466 Castilla, J. C., Manríquez, P. H., & Camaño, A. (2010). Effects of rocky shore coseismic uplift
467 and the 2010 Chilean mega-earthquake on intertidal biomarker species. *Marine Ecology*
468 *Progress Series*, 418, 17-23.

- 469 DeMets, C., Gordon, R. G., & Argus, D. F. (2010). Geologically current plate motions.
470 *Geophysical Journal International*, 181(1), 1–80.
- 471 Fariás, M., Vargas, G., Tassara, A., Carretier, S., Baize, S., Melnick, D., & Bataille, K. (2010).
472 Land-level changes produced by the 2010 Mw8. 8 Chile earthquake. *Science*, 329, 916.
- 473 Grivel, P. F., & Grivel, F. V. (1993). Tablas de Predicción de mareas 1993. Puertos del Pacífico.
474 *Servicio Mareografico Nacional. UNAM*, 115.
- 475 Hjörleifsdóttir V. Sánchez Reyes H. S. Ruiz Angulo A. Ramírez-Herrera M. T. Castillo-Aja R.
476 Singh S. K., and Ji C. 2018. Was the October 9th 1995 Mw 8 Jalisco, Mexico earthquake a
477 near trench event? *J. Geophys. Res.* doi: [https://doi-](https://doi-org.pbidi.unam.mx:2443/10.1029/2017JB014899)
478 [org.pbidi.unam.mx:2443/10.1029/2017JB014899](https://doi-org.pbidi.unam.mx:2443/10.1029/2017JB014899).
- 479 Johansen, H. W. (1971). Effects of elevation changes on benthic algae in Prince William Sound.
480 *In :The Great Alaska Earthquake of 1964, Washington, D.C.: National Academy of*
481 *Sciences*, p.35-68.
- 482 Kostoglodov, V., & Ponce, L. (1994). Relationship between subduction and seismicity in the
483 Mexican part of the Middle America trench. *Journal of Geophysical Research*, 99, 729–
484 742.
- 485 Lagabrielle, Y., Pelletier, B., Cabioch, G., Régnier, M., & Calmant, S. (2003). Coseismic and
486 long-term vertical displacement due to back arc shortening, central Vanuatu: Offshore and
487 onshore data following the Mw 7.5, 26 November 1999 Ambrym earthquake. *Journal of*
488 *Geophysical Research*, 108, 2519.

- 489 Luning, K. S. (1990). *Their environment, Biogeography and Ecophysiology*. New York: John
490 Wiley & Sons, Inc. 527p.
- 491 Melnick, D., Cisternas, M., Moreno, M., & Norambuena, R. (2012). Estimating coseismic
492 coastal uplift with an intertidal mussel: calibration for the 2010 Maule Chile earthquake
493 (Mw= 8.8). *Quaternary Science Reviews*, 42, 29–42, ISSN 0277-3791.
494 <https://doi.org/10.1016/j.quascirev.2012.03.012>
- 495 Ortlieb, L., Barrientos, S., & Guzman, N. (1996). Coseismic coastal uplift and coralline algae
496 record in northern Chile: the 1995 Antofagasta earthquake case. *Quaternary Science*
497 *Reviews*, 15, 949–960.
- 498 Pacheco, J., Singh, S. K., Domínguez, J., Hurtado, A., Quintanar, L., Jiménez, Z., Yamamoto, J.,
499 Gutiérrez, C., Santoyo, M., & Bandy, W. (1997). The October 9, 1995 Colima-Jalisco,
500 Mexico earthquake (Mw 8): An aftershock study and a comparison of this earthquake with
501 those of 1932. *Geophysical Research Letters*, 24, 2223–2226.
- 502 Pacific Tsunami Warning Center. (2020). *ITIC Tsunami Bulletin Board Tsunami, NWs Pacific*
503 *Tsunami Warning Center Bulletin Jun 23 2020, NOAA*. Accessed 23 June 2020.
- 504 Pelletier, B., Régnier, M., Calmant, S., Pillet, R., Cabioch, G., Lagabrielle, Y., Bore, J.-M.,
505 Caminade, J.-P., Lebellegard, P., & Christopher, I. (2000). Le séisme d’Ambrym–Pentecôte
506 (Vanuatu) du 26 novembre 1999 (Mw: 7, 5): données préliminaires sur la sismicité, le
507 tsunami et les déplacements associés. *Comptes Rendus de l’Académie Des Sciences-s-Series*
508 *IIA-e-Sciences de 10 Terre et Des Planetes*, 331(1), 21–28.

- 509 Plafker, G. (1964). Tectonic deformation associated with the 1964 Alaska earthquake. *Science*,
510 148(3678), pp.1675-1687.
- 511 Plafker, G., & Ward, S. N. (1992). Backarc thrust faulting and tectonic uplift along the
512 Caribbean Sea Coast during the April 22, 1991 Costa Rica earthquake. *Tectonics*, 11, 709–
513 718.
- 514 Ramírez-Herrera, M.-T., Corona, N., Cerny, J., Castillo-Aja, R., Melgar, D., Lagos, M.,
515 Goguitchaichvili, A., Machain, M. L., Vazquez-Caamal, M. L., Ortuño, M., Caballero, M.,
516 Solano-Hernandez, E., & Ruiz-Fernández, A. (2020). Sand deposits reveal great
517 earthquakes and tsunamis at Mexican Pacific Coast. *Scientific Reports*, 10, 11452.
518 <https://doi.org/10.1038/s41598-020-68237-2>
- 519 Ramirez-Herrera, M.-T., Kostoglodov, V., Summerfield, M. A., Urrutia-Fucugauchi, J., &
520 Zamorano, J. J. (1999). A reconnaissance study of the morphotectonics of the Mexican
521 subduction zone. *ZEITSCHRIFT FUR GEOMORPHOLOGIE SUPPLEMENTBAND*, 207–
522 226.
- 523 Ramírez-Herrera, M.-T., Lagos, M., Hutchinson, I., Kostoglodov, V., Machain, M. L., Caballero,
524 M., Goguitchaichvili, A., Aguilar, B., Chagué-Goff, C., Goff, J., Ruiz-Fernández, A., Ortiz,
525 M., Nava, H., Bautista, F., Lopez, G. ., & Quintana, P. (2012). Extreme wave deposits on
526 the Pacific coast of Mexico: Tsunamis or storms?—A multi-proxy approach.
527 *Geomorphology*, 139, p.360-371. <https://doi.org/10.1016/j.geomorph.2011.11.002>
- 528 Ramirez-Herrera, M.-T., & Orozco, J. J. Z. (2002). Coastal uplift and mortality of coralline algae
529 caused by a 6.3 Mw earthquake, Oaxaca, Mexico. *Journal of Coastal Research*, 18, 75–81.

Manuscript submitted to Seismological Research Letters

- 530 Sánchez Devora, A. J., & Farreras Sanz, S. (1993). *Catalog of tsunamis on the western coast of*
531 *Mexico. Rep SE-50.*(World Data Center A for Solid Earth Geophysics, NOAA, National
532 Geophysical Data Center, Boulder, Colorado, 1993).
- 533 Servicio Mareográfico Nacional, 2020. Reporte del tsunami producido por el sismo de magnitud
534 7.5 ocurrido el día 23 de junio
535 de 2020 al sureste de Crucecita, Oaxaca. UNAM, México
536 http://www.mareografico.unam.mx/portal/docu/Pdfs/Reporte_Servicio_Mareografico_23_junio_2020.pdf
537
- 538 Servicio Sismológico Nacional (SSN) (2020a) Reporte Especial - Sismo del 23 de Junio de 2020,
539 Costa de Oaxaca (M 7.5). IGEF - UNAM, México.
540 ([http://www.ssn.unam.mx/sismicidad/reportes-](http://www.ssn.unam.mx/sismicidad/reportes-especiales/2020/SSNMX_rep_esp_20200623_Oaxaca-Costa_M75.pdf)
541 [especiales/2020/SSNMX_rep_esp_20200623_Oaxaca-Costa_M75.pdf](http://www.ssn.unam.mx/sismicidad/reportes-especiales/2020/SSNMX_rep_esp_20200623_Oaxaca-Costa_M75.pdf))
- 542 Servicio Sismológico Nacional (SSN). (2020b). *Catálogo de Sismos.*
543 <http://www2.ssn.unam.mx:8080/catalogo/> (Last Accessed June 25, 2020).
- 544 Tait, R. V., & Dipper, F. (1998). *Elements of marine ecology.* Butterworth-Heinemann.
- 545 Trejo-Gómez, E., Ortiz, M., & Núñez-Cornú, F. J. (2015). Source Model of the October 9, 1995
546 Jalisco-Colima Tsunami as constrained by field survey reports, and on the numerical
547 simulation of the tsunami. *Geofisica Internacional*, 54(2), 149–159.
- 548 USGS. (2020). *M 7.4 - 9 km SE of Santa María Xadani, Mexico.*
549 <https://earthquake.usgs.gov/earthquakes/eventpage/us6000ah9t/ground-failure/summary>

Manuscript submitted to Seismological Research Letters

550 *Full mailing address for each author*

551

552 María Teresa Ramírez-Herrera, Laboratorio de Tsunamis y Paleosismología, Instituto de
553 Geografía, Universidad Nacional Autónoma de México. Av. Universidad 3000, UNAM,
554 Coyocán, Ciudad de México, C.P.04510, tramirez@igg.unam.mx

555

556 David Romero H. Facultad de Ciencias, Universidad Nacional Autónoma de México. Av.
557 Universidad 3000, UNAM, Coyocán, Ciudad de México, C.P.04510,
558 dromeroh@ciencias.unam.mx

559

560 Néstor Corona Morales, Centro de Estudios en Geografía Humana-El Colegio de Michoacán,
561 Cerro de Nahuatzen 85, Fracc. Jardines del Cerro Grande, La Piedad, Mich., México, C.P.59379,
562 corona@colmich.edu.mx

563

564 Hector Nava, Dep. de Zoología. Instituto de Investigaciones sobre los Recursos Naturales.
565 Universidad Michoacana de San Nicolás de Hidalgo. Av. San Juanito Itzícuaró S/N, Nueva
566 Esperanza, Morelia Mich. México., C.P.58337, hector.nava@umich.mx

567

568 Hamblet Torija Morales, H. Cuerpo de Bomberos Oaxaca- Blvd. Chahue 1 sector H2, 70980
569 Santa Cruz Huatulco, Oaxaca, Mx, hamblettorija@gmail.com

570

571 Felipe Hernández Maguey, Instituto de Geofísica, UNAM, Circuito de la Investigación
572 Científica s/n, Ciudad Universitaria, Coyoacán, C.P.04510, Ciudad de México,
573 fhmaguey@igeofisica.unam.mx

574

575 **List of Figure Captions**

576

577 Figure 1. Tectonic and earthquake setting. Red bullseye – $M_w > 7$ earthquakes in the Oaxaca
578 region (SSM, 2020b); star – 23 June 2020 epicenter (SSM, 2020a); Moment tensor of the 23
579 June 2020 earthquake (USGS (2020)).

580

581 Figure 2. Vertical zonation of the organisms used in this study.

582

583 Figure 3. Coseismic uplift generated by the La Crucecita M_w 7.4, 23 June 2020, earthquake.
584 Bars indicate the width (m) of the organisms bleached belt (OBB) at 15 locations along 44 km of
585 coastal stretch: 1. San Isidro, 2. Playa del Amor, 3. San Agustín, 4. Bahía Riscalillo, 5. Playa el
586 Órgano, 6. Playa el Violín, 7. Playa Yerbabuena – SEMAR, 8. Playa Pescadores, 9. Fonatur
587 dock, 10. Marina Chahué, 11. Playa Pescadores – Quinta Real, 12. La Bocana Río Copalita, 13.
588 Río Zimatán, 14. Zimatán – Laguna las Garzas, 15. Barra de la Cruz. Blue triangles – sites with
589 values > 0.5 m. Please see the text for explanation.

590

591 Figure 4. Mortality of intertidal organisms caused by sudden land uplift shown by a bleaching
592 belt of intertidal organisms. UL = Upper limit and LL Lower limit of organism bleached belt.

593 a) La Bocana Río Copalita , b) San Isidro, c) Bahía Riscalillo – aerial view of patches of

594 bleached coral reef, d) Marina Chahué, e) Playa el Violín, f) Bleached coral reef at Bahía
595 Riscalillo g) Playa Yerbabuena – SEMAR – bleached coral, h) Playa Pescadores, i). Detail of
596 bleached belt at Playa Pescadores.

597

598 Figure 5. Tsunami runup marked by debris at four locations along the study area. a) El Violín
599 Beach, b) Marina Chahué, c) Playa Yerbabuena – SEMAR.

600

601 Figure 6. Other Geologic effects: liquefaction, fissures, landslides caused by La crucecita
602 earthquake of 23 June 2020. a) Playa Pescadores – Quinta Real, b), c) y g) Zimatán-Laguna las
603 Garzas, d) La Bocana Río Copalita, e), f) Boulevard Chahué.

604

605 Figure 7. Surveying during COVID-19 crisis. A) Arrival at Huatulco airport and reception by the
606 Bomberos de Oaxaca (Oaxaca Firemen). b) SEMAR (Mexican Navy) vessel used to reach
607 inaccessible by land coastal locations. c) Instructions and discussion with SEMAR members
608 keeping a safe distance and wearing masks. d) Sign at Barra de La Cruz indicating restricted
609 access to the town due to COVID-19 confinement.

610

611 **Supplemental material**

612

Manuscript submitted to Seismological Research Letters

Date	Local Hour	Date (UTC)	Hour (UTC)	Elevation (m) (measured from zero Tide Gauge)	Elevation (m) (measured from Mean Sea Level)
25.06.2020	14.45	25.06.2020	19:45	2.112	-0.213
25.06.2020	14.50	25.06.2020	19:50	2.148	-0.177
25.06.2020	15.22	25.06.2020	20:22	2.313	-0.012
25.06.2020	16.32	25.06.2020	21:32	2.670	0.345
25.06.2020	16.39	25.06.2020	21:39	2.680	0.355
25.06.2020	19.47	26.06.2020	00:47	2.870	0.545
25.06.2020	19.56	26.06.2020	00:56	2.880	0.555
25.06.2020	19.57	26.06.2020	00:57	2.880	0.555
26.06.2020	08.20	26.06.2020	13:20	2.690	0.365
26.06.2020	08.25	26.06.2020	13:25	2.660	0.335
26.06.2020	08.28	26.06.2020	13:28	2.650	0.325
26.06.2020	15.15	26.06.2020	20:15	2.090	-0.235
26.06.2020	15.16	26.06.2020	20:16	2.090	-0.235
26.06.2020	15.18	26.06.2020	20:18	2.080	-0.245
26.06.2020	15.47	26.06.2020	20:47	2.200	-0.125
26.06.2020	16.50	26.06.2020	21:50	2.460	0.135
26.06.2020	17.01	26.06.2020	22:01	2.630	0.305
26.06.2020	17.13	26.06.2020	22:13	2.650	0.325
26.06.2020	17.16	26.06.2020	22:16	2.680	0.355
26.06.2020	17.30	26.06.2020	22:13	2.650	0.325
26.06.2020	18.30	26.06.2020	23:30	2.845	0.52

Manuscript submitted to Seismological Research Letters

27.06.2020	11.11	27.06.2020	16:11	2.410	0.085
27.06.2020	11.18	27.06.2020	16:18	2.329	0.004
27.06.2020	11.24	27.06.2020	16:24	2.300	-0.025
27.06.2020	11.28	27.06.2020	16:28	2.300	-0.025
27.06.2020	11.41	27.06.2020	16:41	2.2300	-0.095
27.06.2020	12.28	27.06.2020	17:28	2.160	-0.165
27.06.2020	13.45	27.06.2020	18:45	1.950	-0.375
27.06.2020	14.05	27.06.2020	19:05	1.980	-0.345
27.06.2020	14.36	27.06.2020	19:36	1.890	-0.435
27.06.2020	16.15	27.06.2020	21:15	2.110	-0.215
27.06.2020	20.30	28.06.2020	01:30	2.08	1.037
27.06.2020	21.00	28.06.2020	02:00	2.049	1.006
28.06.2020	10.57	28.06.2020	15:57	1.840	0.797
28.06.2020	11.32	28.06.2020	16:32	1.718	0.675
28.06.2020	11.34	28.06.2020	16:34	1.711	0.668
28.06.2020	12.27	28.06.2020	17:27	1.516	0.473
28.06.2020	12.31	28.06.2020	17:31	1.501	0.458
28.06.2020	12.45	28.06.2020	17:45	1.452	0.409
28.06.2020	13.37	28.06.2020	18:37	1.292	0.249
28.06.2020	13.55	28.06.2020	18:55	1.249	0.206
28.06.2020	16.12	28.06.2020	21:12	1.251	0.208
28.06.2020	18.12	28.06.2020	23:12	1.624	0.581

613

614 Table S1. Tide gauge data from Servicio Mareográfico Nacional (SMN) at Huatulco station.

615 Data were used to assess living position and mortality of intertidal organisms.

616 **Table S2.** Taxonomic identity and vertical zonation of organisms used in this study.

Taxa	Gastropod mollusk	Algae	Barnacle	Barnacle	Polychaete	Bivalve mollusk
Kingdom	Animalia	Plantae	Animalia	Animalia	Animalia	Animalia
Subkingdom	-	Viridiplantae	-	-	-	-
Phylum	Mollusca	Chlorophyta	Arthropoda	Arthropoda	Annelida	Mollusca
Subphylum	-	Chlorophytina	Crustacea	Crustacea	-	-
Superclass	-		Multicrustacea	Multicrustacea	-	-
Class	Gastropoda	Ulvophyceae	Hexanauplia	Hexanauplia	Polychaeta	Bivalvia
Subclass	Neritimorpha		Thecostraca	Thecostraca	Sedentaria	Autobranchia
Infraclass	-		Cirripedia	Cirripedia	Canalipalpata	Pteriomorpha
Subterclass	-		-	-	-	-
Superorder	-		Thoacica	Thoacica	-	-
Order	Cycloneritida	Ulvales	Sessilia	Sessilia	Sabellida	Ostreida
Suborder			Balanomorpha	Balanomorpha	-	-
Superfamily	Neritoidea		Balanoidea	Balanoidea	-	Ostreoidea
Family	Neritidae	Ulvaceae	Balanidae	Balanidae	Serpulidae	Ostreidae
Subfamily	Neritinae		Megabalaninae	Amphibalaninae	-	Crassostreinae
Tribe			-	-	-	-
Genus	<i>Nerita</i>	<i>Ulva</i>	<i>Megabalanus</i>	<i>Amphibalanus</i>	<i>Salmacina</i>	<i>Crassostrea</i>
Species	<i>Nerita scabricosta</i> Lamarck, 1822	<i>Ulva prolifera</i> O.F.Müller, 1778	<i>Megabalanus coccopoma</i> (Darwin, 1854)	<i>Amphibalanus eburneus</i> (Gould, 1841)	<i>Salmacina tribranchiata</i> (Moore, 1923)	<i>Crassostrea corteziensis</i> (Hertlein, 1951)
Vertical zonation	Subtidal and intertidal species, this mollusk grows on hard substrata from above the limit of the highest tides.	Intertidal species, this algae grows from the upper limit of the high tides.	Intertidal species, this barnacle inhabits hard substrata from the upper limit of the high tides up to 100 m depth.	Intertidal species, this barnacle inhabits hard substrata from the upper limit of the high tides.	Intertidal species, this polychaete inhabits hard substrata from the upper limit of the high tides up to 116 m depth.	Intertidal and subtidal species, this mollusk inhabits hard substrata from the upper limit of the high tides.

617

618

619

620

621

622

623

624

625 **Table S2 (continuation).** Taxonomic identity and vertical zonation of organisms used in this study.

Taxa	Bivalve mollusk	Bivalve mollusk	Gastropod mollusk	Vermetid mollusk	Coralline algae	Stony coral	Stony coral
Kingdom	Animalia	Animalia	Animalia	Animalia	Plantae	Animalia	Animalia
Subkingdom	-	-	-	-	Biliphyta	-	-
Phylum	Mollusca	Mollusca	Mollusca	Mollusca	Rhodophyta	Cnidaria	Cnidaria
Subphylum	-	-	-	-	Eurhodophytina	-	-
Superclasses	-	-	-	-	-	-	-
Class	Bivalvia	Bivalvia	Gastropoda	Gastropoda	Florideophyceae	Anthozoa	Anthozoa
Subclass	Autobranchia	Autobranchia	Patellogastropoda	Caenogastropoda	Corallinophycidae	Hexacorallia	Hexacorallia
Infraclasses	Pteriomorpha	Heteromorphia	-	-	-	-	-
Subterclasses	-	Euheteromorphia	-	-	-	-	-
Superorder	-	Imparidentia	-	-	-	-	-
Order	Ostreida	Venerida	-	Littorinimorpha	Corallinales	Scleractinia	Scleractinia
Suborder	-	-	-	-	-	-	-
Superfamily	Ostreoidea	Chamoidea	Lottioidea	Vermetoidea	-	-	-
Family	Ostreidae	Chamidae	Lottiidae	Vermetidae	Lithophyllaceae	Pocilloporidae	Pocilloporidae
Subfamily	Saccostrinae	-	Lottiinae	-	Lithophylloideae	-	-
Tribe	-	-	Lottiini	-	Lithophylleae	-	-
Genus	<i>Saccostraea</i>	<i>Chama</i>	<i>Lottia</i>	<i>Petaloconchus</i>	<i>Lithophyllum</i>	<i>Pocillopora</i>	<i>Pocillopora</i>
Species	<i>Saccostraea palmula</i> (Carpenter, 1857)	<i>Chama coralloides</i> Reeve, 1846	<i>Lottia pediculus</i> (Philippi, 1846)	<i>Petaloconchus complicatus</i> Dall, 1908	<i>Lithophyllum</i> sp.	<i>Pocillopora verrucosa</i> (Ellis & Solander, 1786)	<i>Pocillopora damicornis</i> (Linnaeus, 1758)
Vertical zonation	Intertidal and subtidal species, this mollusk inhabits hard substrata from the upper limit of the high tides.	Intertidal and subtidal species, this mollusk inhabits hard substrata from the upper limit of the high tides.	Intertidal and subtidal species, this mollusk inhabits hard substrata from the upper limit of the high tides.	Intertidal and subtidal species, this mollusk inhabits hard substrata from the upper limit of the high tides.	Subtidal species, this algae grows permanently submerged on hard substrata below the lower limit of the low tides.	Subtidal species, this colonize hard substrata below the lowest limit of the low tide up to 30 m depth.	Subtidal species, this colonize hard substrata below the lowest limit of the low tide up to 30 m depth.

626

627 **Table S2.** Taxonomic identity and vertical zonation of organisms used in this study.

628

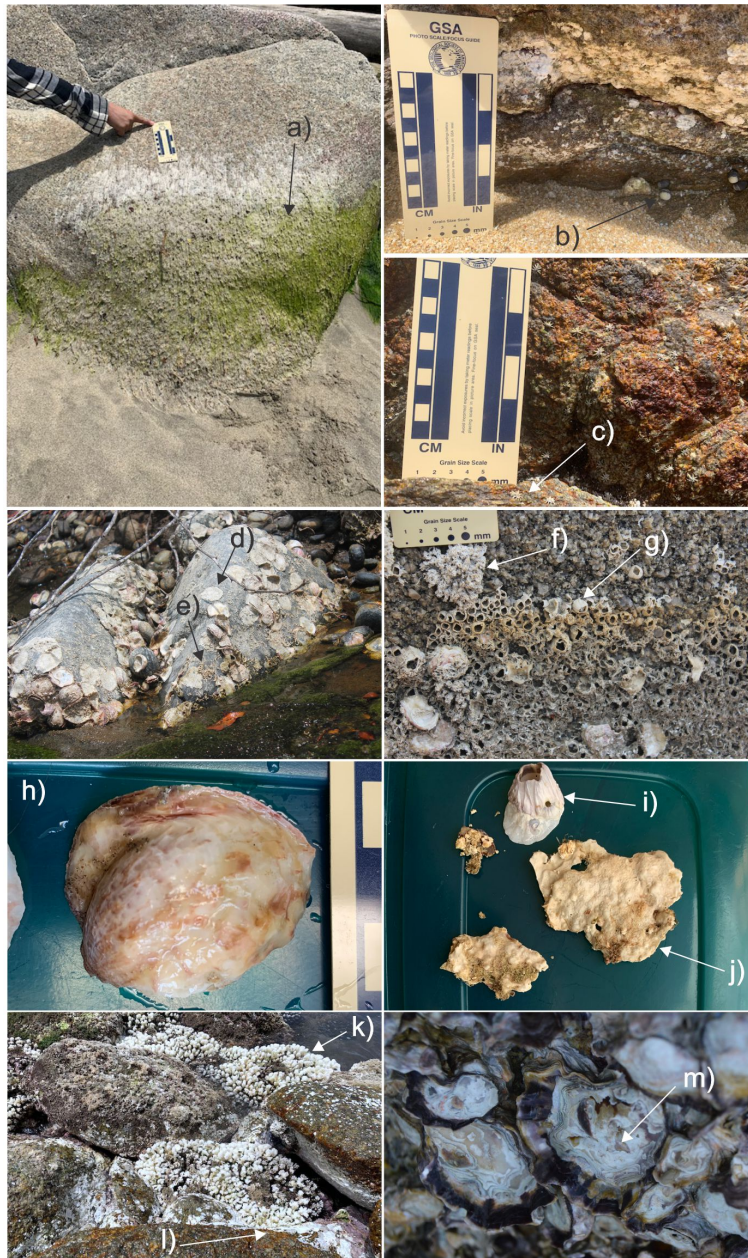


Figure S1. Detail of biomarkers used in this study: a) algae *Ulva prolifera*, b) gastropod *Nerita scabricosta*, c) gastropod *Lottia pediculus*, d) bivalve *Crassostrea corteziensis*, e) vermetid *Petalocochus complicatus*, f) polychaete *Salmacina tribranchiata*, g) crustacean *Amphibalanus eburneus*, h) bivalve *Chama coralloides*, i) crustacean *Megabalanus coccopoma*, j) coralline algae *Lithophyllum* sp., k) stony coral *Pocillopora verrucosa* and l) stony coral *Pocillopora damicornis*, m) bivalve *Saccostrea palmula*.

629

630 Figure S1. Detail of organisms used in this study: a) algae *Ulva prolifera*, b) gastropod *Nerita*

631 *scabricosta*, c) gastropod *Lottia pediculus*, d) bivalve *Crassostrea corteziensis*, e) vermetid

632 *Petalocochus complicatus*, f) polychaete *Salmacina tribranchiata*, g) crustacean *Amphibalanus*

633 eburneus, h) bivalve Chama coralloides, i) crustacean Megabalanus coccopoma, j) coralline
634 algae Lithophyllum sp., k) stony coral Pocillopora verrucosa and l) stony coral Pocillopora
635 damicornis, m) Saccostrea palmula.
636

Tide Gauge – Huatulco, Oaxaca, Mexico

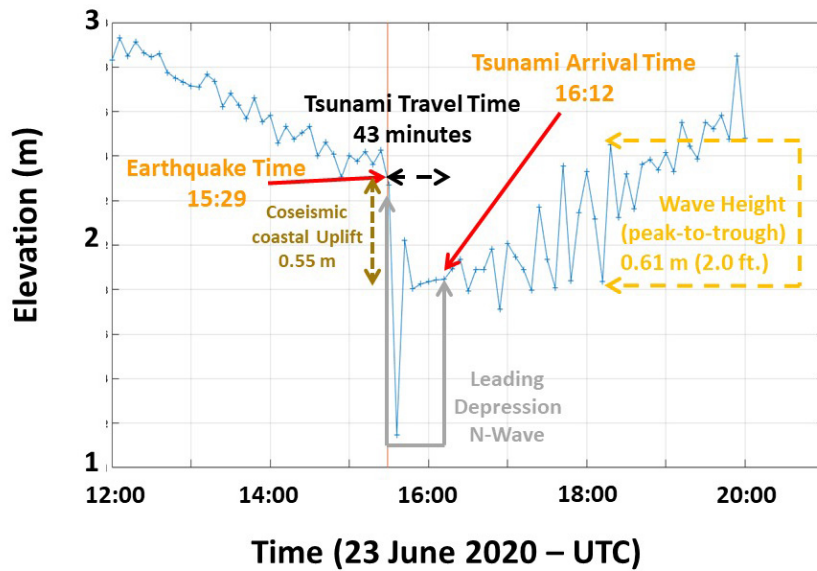


Figure S2. Huatulco tide gauge data interpretation of land level vertical displacement and tsunami amplitude after the 23 June

637
638 Figure S2. Huatulco tide gauge data interpretation of land level vertical displacement and
639 tsunami amplitude after the 23 June 2020 earthquake.